

Czech Technical University in Prague
Faculty of Nuclear Sciences and Physical Engineering

Research work

**Simulation of dilepton cocktail for C+C
at 8 A GeV in HADES**

Jan Novotný

Department of Physics
Academic year: 2003/2004
Supervisor: RNDr. Pavel Tlustý CSc., Nuclear Physics Institute, Czech Academy of
Science, Řež

Prague 2004

Contents

1	Foreword	3
2	Introduction to problematic	5
2.1	Kinematics	5
2.1.a	Particle decays	5
2.1.b	Mandelstam variables	6
2.1.c	Inclusive reactions	7
2.1.d	Invariant mass spectra	7
2.1.e	Transversal momentum	7
2.2	HADES spectrometer	8
2.2.a	RICH	8
2.2.b	MDCs	9
2.2.c	Toroidal magnet	9
2.2.d	TOF	9
2.2.e	TOFino	10
2.2.f	Shower	10
2.3	Dilepton sources	10
3	Simulation of dilepton cocktail	12
3.1	Pluto++	13
3.1.a	Temperature for 2 A GeV	13
3.1.b	Temperature for 8 A GeV	13
3.2	GEANT	14
3.3	HYDRA & ROOT: Make dst procedure	15
3.4	HYDRA & ROOT: Correlator pid	15
3.5	Production multiplicities	17
3.6	Cocktail mixing	20
3.7	Combinatorial background	22
3.7.a	Like-sign pairs	22
3.7.b	Unlike-sign pairs	23
3.8	Acceptance and efficiency	24
3.8.a	Rapidity vs. transversal momentum	26
4	Epilogue	29
4.1	Comparison with The HADES Proposal	29
4.2	Conclusion	29
4.3	Acknowledgment	29

5 Appendix	30
5.1 Software	30
5.1.a UrQMD	30
5.1.b Pluto++	30
5.1.c ROOT	30
5.1.d HYDRA	31
5.1.e GEANT	31
5.2 Examples of scripts	32
5.2.a Pluto++ example	32
5.2.b GEANT script example	33
References	34

Chapter 1

Foreword

This work is concerned on simulation of dilepton invariant mass cocktail for C+C collisions at 8A GeV for the HADES experiment. HADES is a collaboration of 19 groups from 9 countries. The experiment device is placed in GSI, Darmstadt, Germany.

At present stage, Darmstadt accelerator SIS, is able to provide protons with energy 4.5 GeV and heavy ions with 1-2A GeV. However, there exist so called Future Project, a courageous set of improvements and new facilities, that are planned to be done in next ten years. Backbone of this project is new accelerator SIS 200, that could be built up in two phases. First phase supposes available energies around 8A GeV for heavy ions, and this is the reason, we use this energy. Second phase plan to grow up to 30A GeV for medium weight nuclei. This maximum energy was choosed, because the density of nuclear matter, produced in ion-heavy-ion collisions, is estimated to reach a maximal value around 30A GeV. Schematic view of The GSI Future Project is on Figure 1.1.

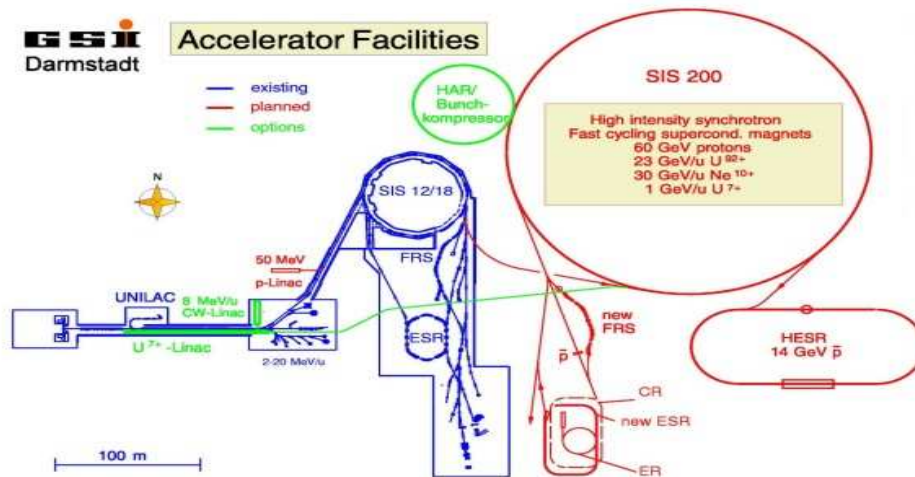


Fig. 1.1: GSI Future Project.

In relativistic heavy ion collision, great amount of energy is released in volume of nucleus order. This heating and warming up leads to hadron gas phase transition. This nuclear phase state consists of nucleons, which behave like free particles.

Recent quark based theories say more. They predict, that increasing energy will lead to the same effect even for quarks. Quark linearly dependent coupling in the hot and dense nuclear phase state, in the quark gluon plasma, will be shadowed by gluons. This effect is usually called restoration of chiral symmetry. In addition, hot and dense nuclear phase state enables to arise processes, which has higher threshold. One of the observable effects connected with the Restoration of Chiral Symmetry and the Quark Gluon Plasma creation is production suppression of J/Ψ relative to the hadron gas.

Another important feature connected with restoration of chiral symmetry is change in the rest mass of particles “living” in hot and dense environment. This effect is briefly depicted on Figure 1.2. Variable $\langle \bar{q}q \rangle_{\rho,T}$ is quark condensate. The mass of mesons has monotonously increasing dependence on quark condensate. More can be found in [ChSR].

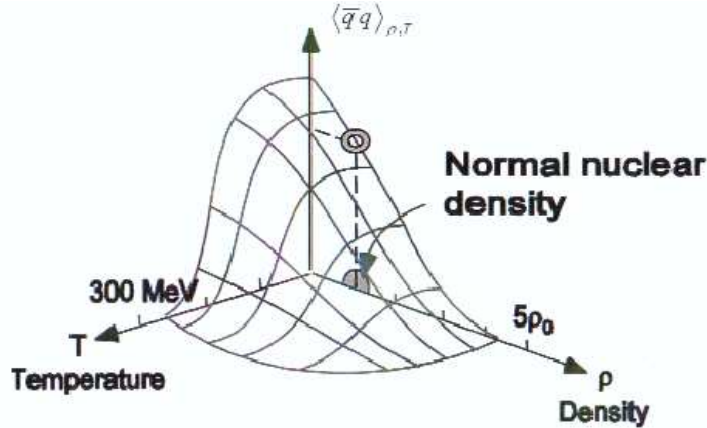


Fig. 1.2: Quark condensate on the temperature and the density dependency.

To study properties of changing rest mass, or invariant mass, we need to get information about mass of particles in hot and dense matter. The way, how to do it, is in nuclear physics via decays. Thus we need particle decay in medium and also need to detect decay product. As the best tool for this work seems to be decay of vector mesons through the dilepton channel. The ideal mesons are ρ , ω and ϕ . Especially the first listed, ρ meson, with his lifetime $t_{life} \approx \text{fm}/c$ is suited for study of in-medium properties. HADES detector was built up to study dileptons, e^+e^- pairs originating from heavy-ion collisions. Post analysis should give the information about invariant mass spectra of sources in the reaction.

Invariant mass spectra simulation at 8A GeV for C+C system was main aim of this work. There exists a plan, that HADES detector will be used in the first phase of the GSI Future Project. This first phase, as was mentioned above, will get energy range up to 8A GeV. This work should give first answer whether the present HADES setup is useful in higher energy range and, alternatively, to show, what improvements have to be done for getting better acceptance (changing geometrical setup, in reality, it is possible only to move the sub-detectors in beam direction, or exchange some sub-detector for newer one, e. g. often discussed time-of-flight detector system).

The electromagnetic structure of mesons and baryons can be studied through their time-like form factors. Its knowledge is important in any modeling of hadrons. Transition form factors can be calculated from the dilepton invariant mass spectra. Interesting channels are in this case Dalitz decays on neutral meson, γe^+e^- or $\gamma\gamma e^+e^-$.

Chapter 2

Introduction to problematic

In the first part of this chapter, we would like to give a very short introduction to the kinematics, especially the terms used or interrelated with my work are explained here. Then few words about invariant mass spectra, transversal momenta and temperature will follow. Chapter continue with with description of HADES spectrometer. Then the dilepton sources used in simulation are shortly presented.

2.1 Kinematics

In this part, we will pin out some pieces of the basics of kinematics. More can be found in each course book on the kinematic or [Pdg].

2.1.a Particle decays

The decay of particle with mass m and momentum P into n products, each with momentum p_i , is given by

$$d\Gamma = \frac{(2\pi)^4}{2m} |M|^2 dLIPS_n, \quad (2.1)$$

where M is Lorentz-invariant matrix element and $dLIPS_n$ is n -body Lorentz Invariant Phase Space element defined as

$$dLIPS_n = \delta^4(P - \sum_{i=1}^n p_i). \quad (2.2)$$

Two-body decay

Two-body decay is depicted on Figure 2.1. Particle decay rate can be given

$$d\Gamma = \frac{1}{32\pi^2} |M|^2 \frac{|p_1|}{m^2} d\Omega, \quad (2.3)$$

where $d\Omega$ is the solid angle of the first particle and for kinematical variables hold following two relations

$$E_1 = \frac{m^2 - m_2^2 + m_1^2}{2m}, \quad (2.4)$$

$$|p_1| = |p_2|$$

$$= \frac{[(m^2 - (m_1 + m_2)^2)(m^2 - (m_1 - m_2)^2)]^{1/2}}{2m}. \quad (2.5)$$

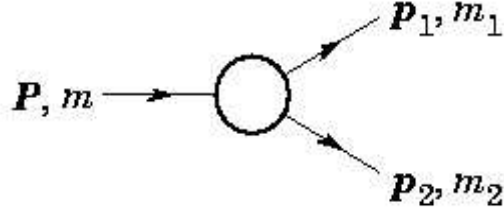


Fig. 2.1: 2-body decay process scheme.

Three-body decay

Three-body decay process is shown on Figure 2.2. Particle decay rate is given

$$d\Gamma = \frac{1}{2\pi^5} \frac{1}{16m^2} |M|^2 |p_1^*| |p_3| dm_{12} d\Omega_1^* d\Omega_3, \quad (2.6)$$

where $(|p_1^*|, \Omega_1^*)$ is the momentum of the first particle in the rest frame of 1 and 2, Ω_3 is the angle of the particle 3 in the rest frame of the decaying particle. Used kinematical variables satisfy following relations

$$m_{12}^2 = (P - p_3)^2, \quad (2.7)$$

$$|p_1^*| = \frac{[(m_{12}^2 - (m_1 + m_2)^2)(m_{12}^2 - (m_1 - m_2)^2)]^{1/2}}{2m_{12}}, \quad (2.8)$$

$$|p_3| = \frac{[(m^2 - (m_{12} + m_3)^2)(m^2 - (m_{12} - m_3)^2)]^{1/2}}{2m}. \quad (2.9)$$

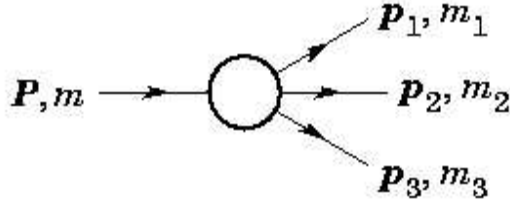


Fig. 2.2: 3-body decay process scheme.

2.1.b Mandelstam variables

It use to be very useful to define in two-body reactions the Mandelstam Lorentz-invariant variables

$$\begin{aligned} s &= (p_1 + p_2)^2 = (p_3 + p_4)^2 \\ &= m_1^2 + 2E_1E_2 - 2p_1 \cdot p_2 + m_2^2, \\ t &= (p_1 - p_3)^2 = (p_2 - p_4)^2 \\ &= m_1^2 - 2E_1E_3 + 2p_1 \cdot p_3 + m_3^2, \\ u &= (p_1 - p_2)^2 = (p_2 - p_3)^2 \\ &= m_1^2 - 2E_1E_4 + 2p_1 \cdot p_4 + m_4^2. \end{aligned} \quad (2.10)$$

These variables satisfy following relation

$$s + t + u = m_1^2 + m_2^2 + m_3^2 + m_4^2. \quad (2.11)$$

We remind, for completeness' sake, the sign A GeV mean energy per nucleon.

2.1.c Inclusive reactions

We choose the z -axis same as the beam direction, then the energy-momentum four vector can be cast to the form:

$$(p_0, p_1, p_2, p_3) = (m_T \cosh y, p_x, p_y, m_T \sinh y), \quad (2.12)$$

where the transverse mass m_T is defined as

$$m_T^2 = m^2 + p_x^2 + p_y^2, \quad (2.13)$$

and the rapidity y

$$y = \frac{1}{2} \ln \left(\frac{E + p_z}{E - p_z} \right) = \ln \left(\frac{E + p_z}{m_T} \right) = \tanh^{-1} \left(\frac{p_z}{E} \right) \quad (2.14)$$

Transverse momentum p_T can be defined as

$$p_T = p_x + p_y. \quad (2.15)$$

Under a boost in the z -axis to a frame with velocity $\beta = v_{boost}/c$, rapidity change $y \rightarrow y - \tanh^{-1} \beta$.

2.1.d Invariant mass spectra

The rest mass of products is not equal to mass of decayed particles in decay processes. If we want to know rest mass of source, we have to calculate invariant mass. This variable is Lorentz invariant, i. e. it is independent on the given frame. Invariant mass is defined as

$$m_{inv}^2 = (\sum E_i)^2 - (\sum p_{ix})^2 - (\sum p_{iy})^2 - (\sum p_{iz})^2, \quad (2.16)$$

where E_i and p_i are produced particles' energies or momenta, respectively.

The invariant mass spectra, we get, say us the rest mass of decayed particles. It is true in two particle decay. In our case, we have also three particle Dalitz decay, where we have the information only from two of the three particles. Thus our invariant mass spectrum will not be peaked around the rest mass, but it will starts at zero mass and will continue up to invariant mass value. Examples of this will be seen in the final dilepton cocktail.

2.1.e Transversal momentum and temperature

In heavy-ion collision at energies used in GSI (1-2A Ge V present, up to 8A Ge V planned) the nuclear medium can be compressed up to many times the normal nuclear matter density. The reaction zone of incident nucleons and produced particles is hot and dense. The thermal model approach assumes, that nuclear medium form an ideal gas, which at high temperature expands like a exploding fireball. This effect leads to hadronic freeze-out.

If the thermal model is valid, transverse mass, m_T , spectra measured at mid-rapidity can be approximately described by Maxwell-Boltzmann distribution:

$$\frac{1}{m_T^2} \frac{dN}{dm_T} \propto \exp(-m_T/T), \quad (2.17)$$

where the inverse slope parameter T , temperature, corresponds to a temperature of freeze-out of the particles emitting by gas-source and m_T is defined:

$$m_T = \sqrt{p_T^2 + m^2}, \quad (2.18)$$

and transverse momentum, p_T , is the transverse part of the momentum vector. I have used this approach in my work.

The sophisticated approach implementing thermal model use two different temperatures, T_1 and T_2 , each with appropriate weight, C_1 and C_2 . Appropriate equation stands

$$\frac{1}{m_T^2} \frac{dN}{dm_T} = C_1 \exp(-m_T/T_1) + C_2 \exp(-m_T/T_2). \quad (2.19)$$

2.2 HADES spectrometer

High **A**cceptance **D**i-**E**lectron **S**pectrometer is high-end magnetic spectrometer for high momentum resolution measurement of electron-positron pairs. It was constructed for relativistic ($\gamma > 1$) heavy ion collisions at energy regimes 1-2A GeV. Spectrometer has to be able to select leptons among dozens of times more hadrons arising from reactions. In addition to selective role, it has to be able to measure their energy with sufficient accuracy. The key features of The HADES spectrometer are:

- a. A large geometrical acceptance (40%) in combination with an advanced count rate capability ($\approx 10^6$ reactions per second).
- b. A resolution for invariant mass reconstruction comparable to the natural width of the ω meson ($\sigma_M/m \approx 1\%$)
- c. A signal-to-background ratio significantly larger than unity up to invariant masses $m \approx 1 \text{ GeV}^{-2}$.
- d. An excellent lepton to hadron discrimination.
- e. A high granularity to cope with heavy collision systems.

Figures 2.3 and 2.4 show The HADES setup. It has hexagonal construction shape and covers polar angles from 18° up to 85° . Its main parts are (as follows in beam direction): **R**ich **I**maging **C**herenkov detector, first two layers of **M**ulti-**W**ire **D**rift **C**hambers, toroidal magnets, last two layers of **M**DC, **T**ime-**O**f-**F**light detectors, low polar angle Time-Of-Flight detector **T**O**F**ino and finally **S**HOWER detector. Short description follows below.

2.2.a RICH

The main purpose of **R**ich **I**maging **C**herenkov detector is identification of electrons and positron from the larger hadron background arisen from interaction of colliding particle with target. There is several order of magnitude difference in production of hadrons and leptons in heavy system collisions.

In The HADES energy regimes, electrons and positrons have the velocity nearly equal to the velocity of light ($\beta \approx 1$) while hadrons has velocity lower ($\beta \leq 0.95$). It is possible to choose appropriate filling gas to get emission of Cherenkov radiation in the detector only for those particles, which have velocity of electron (we take into account only those hits, which fullfil $\beta \leq 0.9985$).

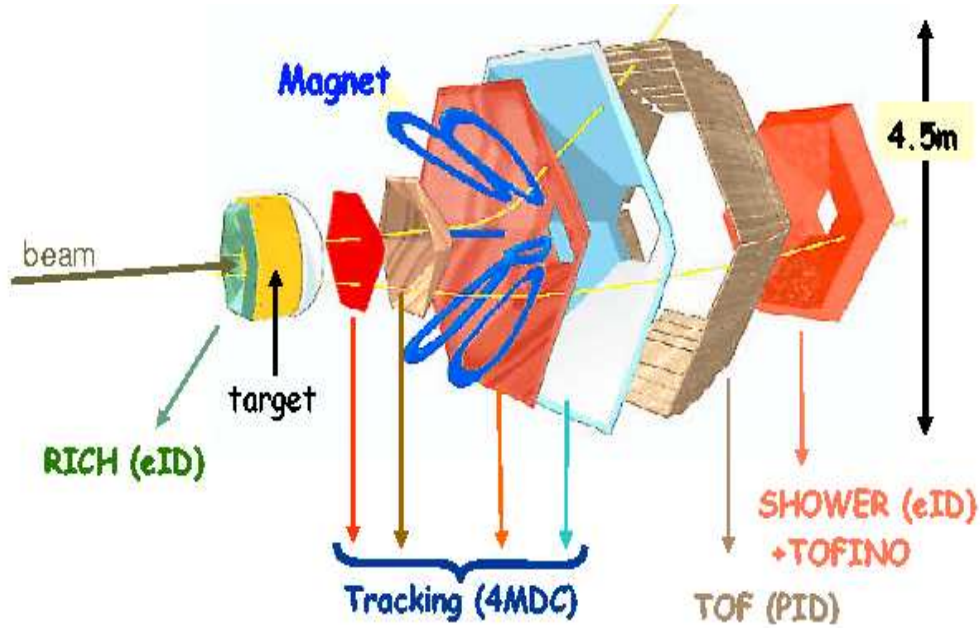


Fig. 2.3: HADES setup

Radiator gas is C_4F_{10} at working pressure 1000–1200 h Pa. Cherenkov radiation of all polar angles is reflected and focused with one spherical mirror (made of pure carbon) on the photon detector. Mirrored rings has roughly equal diameter (≈ 5 cm). More can be found in [Www].

2.2.b MDCs

Four Multi-Wire Drift Chambers are used for particle tracking. Each chamber consists of six layers of anode and cathode wires. Chambers are placed to contain approximately right angle with the trace of particles. Position resolution of this system is lower than $100 \mu\text{m}$. Size of cells inside the chambers differs from 5×5 mm to 10×14 mm to have a constant granularity. Chambers are filled with $He - iC_4H_{10}$.

2.2.c Toroidal magnet

Toroidal magnet has six parts each placed in independent vacuum chambers. It is able to reach magnetic field intensity 0.7 Tesla. It is sufficient for momentum measuring of charged particles with accuracy of 1%.

2.2.d TOF

Time-Of-Flight detector consist of 384 scintillator rods situated in six sectors. Rods are placed in modules (with eight rods each). TOF covers polar angles from 44° to 88° . Rods have square profile with 20×20 mm (low polar angles and therefore higher multiplicity) and 30×30 mm diameter. Each rod ends with two photomultiplier. It has time of flight resolution (sigma) lower than 150 ps. The total time of converting signal from analog to digital form is lower than $10 \mu\text{s}$.

Main purposes of TOF chambers are:

- A measuring of time of flight of particles.
- A fast estimation of multiplicity in reaction for triggering purposes

c. A fast estimation of particle direction of flight for triggering purposes.

2.2.e TOFino

From economical reasons are for polar angles lower than 44° TOF chambers changed with **TOFino**. Each of six sectors of TOFino system, consists of four delta-shaped scintillators placed below, in the sense of beam direction, the SHOWER detector. Each of this scintillator has one photomultiplier. The time resolution (sigma) of TOFino is around 450 ps. Ability of trace measuring is significantly lower than in the TOF case. It is supposed to be TOFino replaced with RPC walls. More can be found in talks from Catania meeting on [Www].

2.2.f SHOWER

SHOWER detector is based on the measuring electromagnetic showers produced by electrons and positrons in medium with high proton number. It consists of three wire chambers and two lead converters sandwiched between each two wire chambers.

The reason of SHOWER usage is because of high production ratio of leptons in low polar angles and high β of hadrons in the same angles, therefore the identification efficiency via RICH and TOF detectors is decreased.

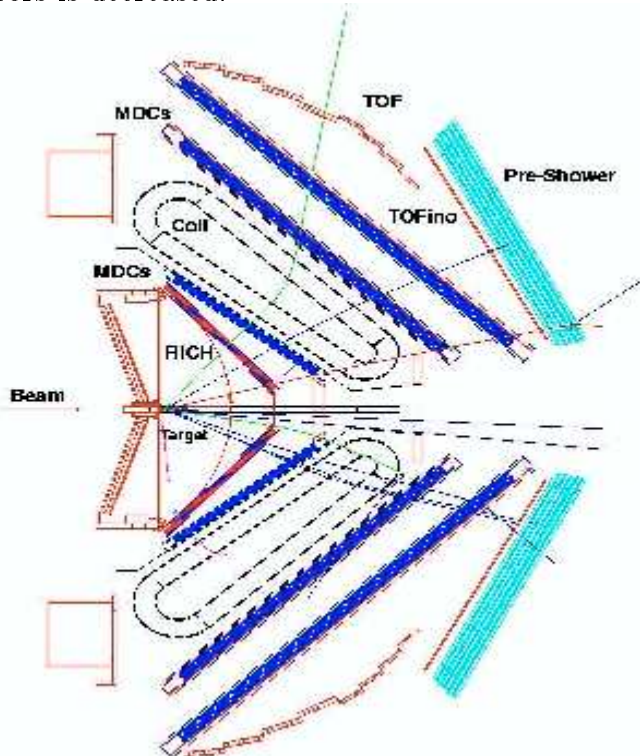


Fig. 2.4: HADES setup, cross section view.

2.3 Dilepton sources

As was mentioned above, we concern on properties of vector meson (ρ , ω , ϕ , *eta*) decays via dilepton (electron-positron) channel. One question immediately arises: Are there any dilepton sources in addition to vector meson decays in heavy ion collision? Unfortunately, the answer is yes. We have take into account also the neutral π decay channel, and the δ resonance decay channel.

Short description of electron-positron decay channels, we have used, follows [Pdg]. For each process, we have listed in the following Table 2.1 basic characteristic of source particles

as mass and branching ratio for each dilepton channel. We would like to remind, that branching ratio is only one of the characteristic, that says us, how significant is given channel. Production ratios, second significant characteristic of decay channel, of source particles will be discussed in the next chapter.

Sources were choosed same as in The HADES Proposal [Hpr]. The only exception is *pn-bremsstrahlung*. The Proposal use it, i. e. at 2A GeV energy regime ,however, it is not possible to make a qualified estimate of total production ratio in the 8A GeV case, because it is not possible distinguish channels via Δ resonance and *pn-bremsstrahlung*. We have decided to not take into account this source. Values were taken from [Plt].

Channel	mass [Me V]	BR
$\pi^0 \rightarrow \gamma + e^+ + e^-$	134.97	0.0119
$\eta \rightarrow \gamma e^+ + e^-$	547.30	4.9×10^{-3}
$\omega \rightarrow \pi^0 + e^+ + e^-$	782.57	5.9×10^{-4}
$\omega \rightarrow e^+ + e^-$	782.57	7.1×10^{-5}
$\rho \rightarrow e^+ + e^-$	771.1	4.5×10^{-5}
$\phi \rightarrow e^+ + e^-$	1019.45	2.9×10^{-4}
$\Delta \rightarrow N + e^+ + e^-$	≈ 1232	3.3×10^{-5}

Table 2.1: Overview of BR's and masses used in simulation.

Chapter 3

Simulation of dilepton cocktail

In this chapter, we would like to describe process of simulating dilepton cocktails, i. e. electron-positron pair arisen in heavy ion collision. In our case, we have simulated C+C nuclear system at energies 2A Ge V and 8A Ge V . The whole process schematically describes next Figure 3.1.

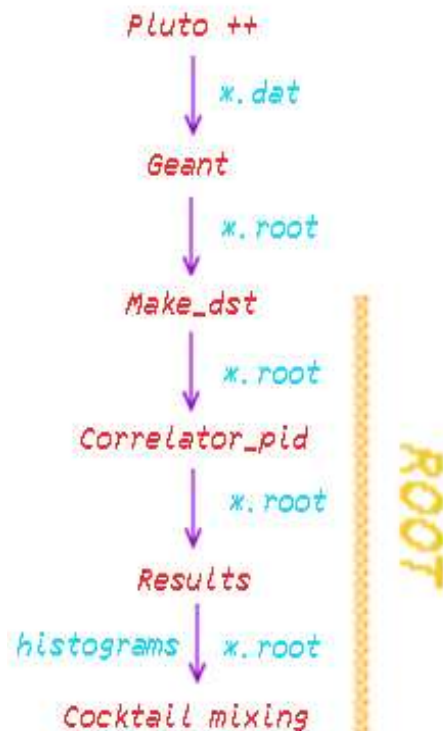


Fig. 3.1: Schematic of dilepton cocktail simulation.

At the beginning of the simulation process, we have to choose the system, we will simulate. C+C collision was choosed, because was studied for former HADES proposal and was recently measured by HADES. Estimated particle production for 8 A Ge V will be in permissible allowance. Although we want higher multiplicities of dielectron pairs, we have to take into mind, that not only dileptons are produced in collisions. Apart from them, hadrons are produced. They are also interacting with detector and could significantly decrease the efficiency of dilepton detection.

Next step is to choose dielectron sources, we will use. They were briefly mentioned above.

Pluto simulation follows. We have produced 50 thousand events for every source. We have choosed the way, where particular sources are propagated through the whole process separately until the “measured” invariant mass spectra is done. Then component spectra

are getting together.

Next step is GEANT simulation of decay products in the detector.

HYDRA turns come on the scene. It consists of producing *.dst files, i. e. files we get after the Data Acquisition for analyzing.

Finally, invariant mass cocktail can be mixed with appropriate multiplicities. To this ideal result pairs-events, that not originate from one source decay but from random coupling of electrons and positrons have to be added. This is usually called combinatorial background. Detailed disscusion of above foreshadowed scenario follows.

3.1 Pluto++

We have used Pluto++ version 3.06. Generating of decay products (e^- , e^+ and γ , in my case) was based on thermal bath approach, i. e. isotropical fireball expansion of source. It implies, it is necessary to choose appropriate temperature of the fireball (more about thermal model and temperature was given above). Finding of temperature follows in next two subsections.

For better simulations of real processes, this thermal approach contains additional boost of fireball expansion. We have used value of the expansion velocity 0.3 . More about Pluto++ input parameters can be found in [Plt].

As I mentioned, we have produced for every dilepton source 50 thousand events. Output of this process serves as an input for GEANT processing.

Example of production macro of dileptons from η thermal source at 8A Ge V is attached in Attachment section at the end of this work.

3.1.a Temperature for 2A GeV

We have choosed temperature 89 Me V, because the same temperature was used for [Hpr]. Overview of measured temperatures in other experiments for 2A Ge V energy regimes follows in Table 3.1 as well as our value, we have got from UrQMD. We have used UrQMD to produce 50000 events of C+C collisions at 2A Ge V and then fit transversal momenta of pions.

Experiment	temperature [Me V]
HADES proposal	89
TAPS exp. value for π	83 ± 2
KAOS exp. value for π	86 ± 3
UrQMD fit	86 ± 1

Table 3.1: Overview of temperatures measured in various experiments for 2A Ge V .

3.1.b Temperature for 8A GeV

We have used temperature 105 Me V . We have got this value by fitting the transversal momenta of pions at 8A Ge V produced by UrQMD code in C+C system (105 ± 1 Me V). Spectrum of transversal momenta of π used for fitting is depicted on Figure 3.2, where x -axis represent transversal momenta. You can see strong exponential decrease from x -values above cca 0.3 .

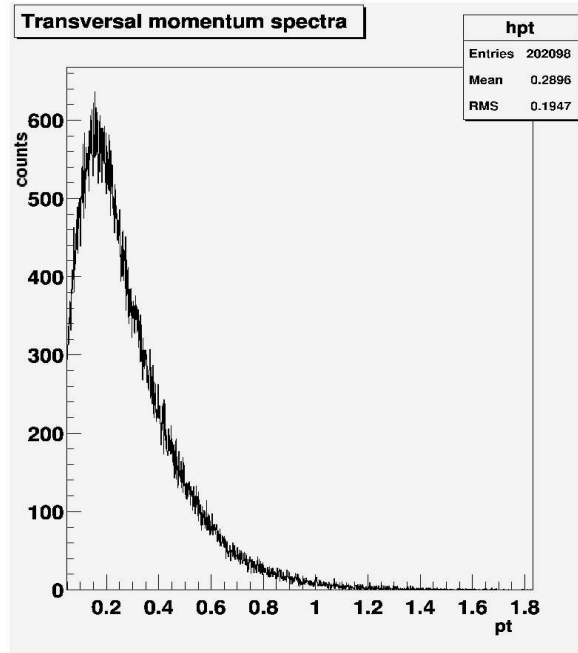


Fig. 3.2: Spectrum of transversal momenta of π produced by UrQMD at 8A Ge V in C+C system.

We tried to study, how change the acceptance of dileptons on various temperatures for thermal source of η in the HADES. We have produced in Pluto++ 50000 events for every energy regime and applied geometrical filter. Table 3.2 shows dependency of refused pairs on energy. The acceptance (filter) was taken just in the geometrical manner, i. e. $18^\circ < \theta(e^+) < 85^\circ$ and $18^\circ < \theta(e^-) < 85^\circ$. It seems, that the acceptance does not significantly depend on the temperature of the thermal source.

Temperature [Me V]	Events refused
100	23507
105	23540
110	23542
115	23561
120	23560
150	23543

Table 3.2: Table shows dilepton acceptance of the HADES for η thermal source at 8A Ge V for various temperatures.

Usage of weighted temperatures, equation (2.9), did not result differently.

3.2 GEANT

As a next step in the production of dilepton cocktail is GEANT analysis. Collection of packages implemented into GEANT for HADES purposes is called HGEANT. We have used version version3_13. This GEANT procedure simulate propagation of particles in HADES

spectrometer. Particles, produced in the thermal or whatever else model, are uniformly situated in the volume of target. Then GEANT simulates its interaction with detector system, it mean with the detector active volume as well as with the construction and support facilities contained in the cave (protected room, where the spectrometer is situated). Interaction with active parts of the detector gives us appropriate response in electronics, however output from HGEANT just says, there is an interaction of this kind, it is not responsible for simulating of evolution of electronic pulses in Data Acquisition system. The GEANT also simulates propagation of secondary (and higher generation) particles emitted in the detector volume.

3.3 HYDRA & ROOT: Make dst procedure

Section about HYDRA follows. We have used HYDRA version 'nov01 sim gen5'. What we call here "Make dst" procedure is responsible for producing output "same as from the experiment". This phrase mean two phases of processing raw GEANT data. First stage means using of "digitizers", be specific, the translation of GEANT values to the language of electronics, i.e. energy is converted to channels. Second phase is "calibration", i.e. converting of channel values into the physical numbers using calibration setup same as in experiment. It seems to be pointless, however, we get the output in the same way as Data Acquisition gets it from the experiment. In this stage, we can select, what parts of the detector setup will be switched on and what will be switched off. In the case of simulations, we can use parts of detector, that are not physically implemented, but implemented in software tools. It was my case, when we have used 3 MDC chambers. The same setup was used in experiment C+C in NOV2001. It was possible even to use 4 MDC chambers.

3.4 HYDRA & ROOT: Correlator pid - Particle Identification

Correlator pid part of analyzing data mean selecting events and calculating its properties from informations, we have measured-simulated in the experiment. In the reconstruction of invariant mass spectra process, we are concerned on identifying electron-positrons pairs originated from primary channels, and measuring its properties, in particular its track, momentum, charge and rich response (if any).

For decision, whether the registered particle is electron or positron, we have used following criteria:

$$\begin{aligned} \text{charge} &= \pm 1 \\ \text{RICH response} &= \text{positive} \\ \text{parent flag} &= \text{decay of oroginal part.} \end{aligned} \tag{3.1}$$

In addition to this conditions, the GEANT ID was checked. It was clear from results, that identification via (3.1) was in very good agreement with GEANT ID flag. Parent flag condition was used because of affirmation, that the particles originate from original particle decay.

In the present setup, it was not possible to use 3MDC's simulation to measure momentum, thus we have used GEANT momentum value. However, it was necessary to smear this value for more realistic description of collision. Smearing function was taken from [Jar] and reads:

$$\frac{\Delta p}{p} = (1 + 3.6p)\%, \quad (3.2)$$

Next step is identification of dielectron pairs:

$$e^+e^- \text{ angle} \geq 5^\circ \quad (3.3)$$

$$\text{number of primary products} = 2$$

Opening angle was used same as in [Hpr], more note about this can be found in Conclusion. Main reason was to suppress e^+e^- pairs from other processes, especially from $\gamma \rightarrow e^+ + e^-$, where the opening angle is small. We have also mentioned limits of distinguishing too close pairs. They can have the same hit in sub-detectors close to target (between target and magnet), or on the other hand, one hit in e. g. inner MDC can be attached to real particle and also can be joined to any independent hit in outer chamber. As a result, we get a pair. However, this pair does not exist. We have also tested condition with 15° . Multiplicity of registered pairs decreased, but seemed to be not necessary to use this higher value.

Finally, the invariant mass histograms is filled. We can recast definition of the invariant mass (2.16) into the form:

$$m_{inv} = \sqrt{2p_{e^+}p_{e^-}(1 - \cos(\alpha_{e^-e^+}))}, \quad (3.4)$$

where p_{e^-,e^+} are the electron and positron momenta and $\alpha_{e^-e^+}$ is their opening angle. Masses of electrons were neglected.

Examples of the invariant mass spectra from η Dalitz decay channel follow on Figures 3.3 and 3.4.

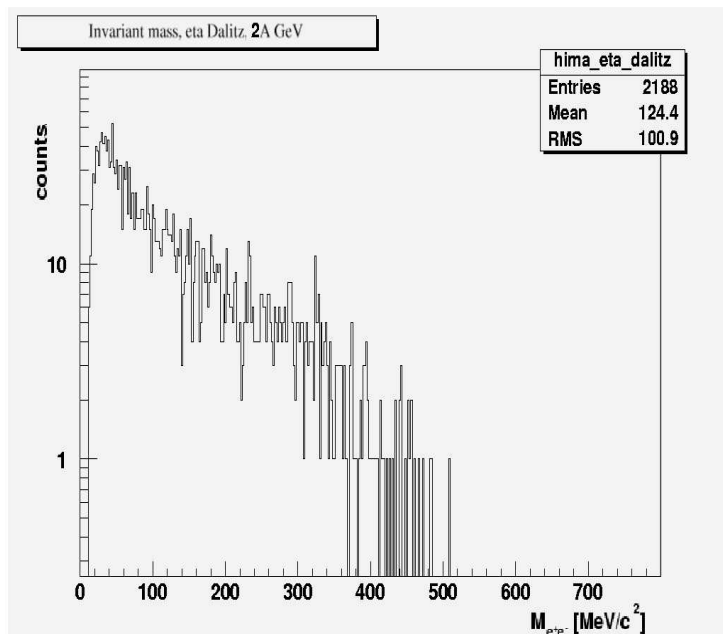


Fig. 3.3: Invariant mass spectrum for η Dalitz decay channel for 2A GeV . Y-axis is log scaled.

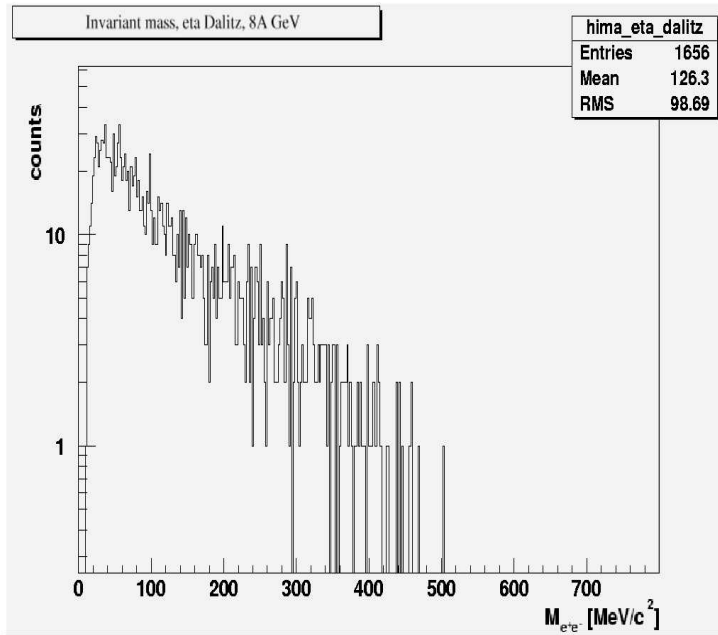


Fig. 3.4: Invariant mass spectrum for η Dalitz decay channel for 8A GeV . Y-axis is log scaled.

3.5 Production multiplicities

To mix a dielectron invariant mass cocktail, it is necessary to know source particle production multiplicity per one nucleus-nucleus collision and branching ratio of a given source. Product of these two numbers gives us a ratio of importance. If we multiply this number by average number of collisions in one run (or time, which HADES has available beam from accelerator), we have the number of pairs, we have available in one run from given source. The total number of registered pairs depends on detection conditions, i. e. it decreases because of acceptance and efficiency of the detector. More on this topic will be discussed below.

The HADES detector use multilevel triggering system [Pos], which enables us to select more central collisions, i. e. events, where more than average number of nucleons collide and therefore more particles is produced. We have used 39% more central collision setup, which gives us 12 participants (nucleons) per collision. For the sake of completeness, minimum bias correspond to 6 participants.

Nucleon-nucleon production multiplicities at 2A GeV were taken the same as in the proposal. The case of 8A GeV was more complicated. It is not possible to get any experimental data, thus it was necessary to make any qualified estimation. We have used data produced from thermal model made by Anton Andronic in GSI [Ant]. Yields of η , ω and ϕ to $\pi^+ + \pi^-$ are on Figure 3.5. I have read values from this chart at $\sqrt{s} = 2.6$ GeV for 2A GeV and $\sqrt{s} = 4.3$ GeV for 8A GeV . This values gave the ratio between production at 2 and 8A GeV . This ratios are shown in the Table 3.3.

meson kind	ratio
η	7.9
ω	310.4
ϕ	108.3

Tab. 3.3: Ratios of production multiplicities for 2 and 8 A Ge V . Data given from Fig. 3.5.

Multiplicities for 8A Ge V was given as

$$\text{Mult}_{8A \text{ Ge V}} = \text{Mult}_{2A \text{ Ge V}} \times \text{ratio}. \quad (3.5)$$

\sqrt{s} is given by

$$s = 4m_N^2 + 2m_N E_{kin}, \quad (3.6)$$

where m_N is the mass of nucleon and E_{kin} is energy per nucleon.

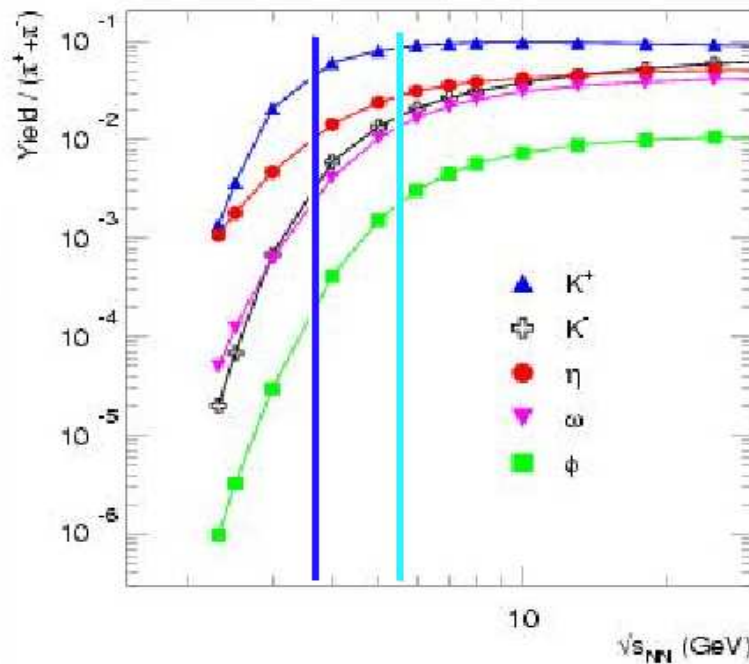


Fig. 3.5: Vector meson yields (relatively to $\pi^+ + \pi^-$) dependence on \sqrt{s} . Dark blue vertical line relates to 2 A Ge V ($\sqrt{s} = 2.6$ Ge V) and light blue line relates to 8 A Ge V ($\sqrt{s} = 4.3$ Ge V).

Data for π were measured by E895 [Kla]. We have took their final published ratio 4.123 and multiplicity was given by equation (3.5).

The ratio for Δ resonance was given by estimation, that Δ multiplicity of Δ is 1.5 times larger than in the pion case. This value was used for the proposal.

Ratio for ρ was estimated in the same way as was done in [Ave]. There are estimates in the region around 2 A Ge V and these was extrapolated to higher energies. The ratio is 75.0 and we again use equation (3.5). This is the worst estimation among all listed above.

Production multiplicities used in simulation for each particular source of dileptons per collisions (i. e. multiplied by number of participants in collision) are listed in Table 3.4. There are also the same values multiplied by the Branching Ratios (see above).

source	Mult. ²	$M_{e^+e^-}^2$		Mult. ⁸	$M_{e^+e^-}^8$
π^0 Dalitz	1.71	2.0×10^{-2}		7.05	8.3×10^{-2}
η Dalitz	4.3×10^{-2}	2.1×10^{-4}		0.34	1.6×10^{-3}
ω Dalitz	4.8×10^{-3}	2.8×10^{-6}		1.49	8.6×10^{-4}
ω direct	4.8×10^{-3}	3.4×10^{-7}		1.49	1.1×10^{-4}
ρ direct	4.8×10^{-3}	2.1×10^{-7}		0.36	1.6×10^{-5}
ϕ direct	4.8×10^{-4}	1.3×10^{-7}		5.2×10^{-2}	1.5×10^{-5}
Δ Dalitz	2.56	8.4×10^{-5}		10.57	8.2×10^{-7}

Tab. 3.4: Production ratios per collision and same values multiplied by Branching Ratios of particular sources for 2 and 8 (upper index) A Ge V .

3.6 Cocktail mixing

The procedure described above was done for each source. Finally, the dilepton cocktail was mixed. The particular invariant mass spectra were normalized to one collision and then summed together. It means that final spectrum was before completing multiplied by the production ratio (production multiplicity times branching ratio times average number of participants) and divided by number of events used for producing (as stated above, we have used 50 thousand collisions per source). On the following two Figures 3.6 and 3.7 are the total invariant mass spectra for 2 and 8A Ge V .

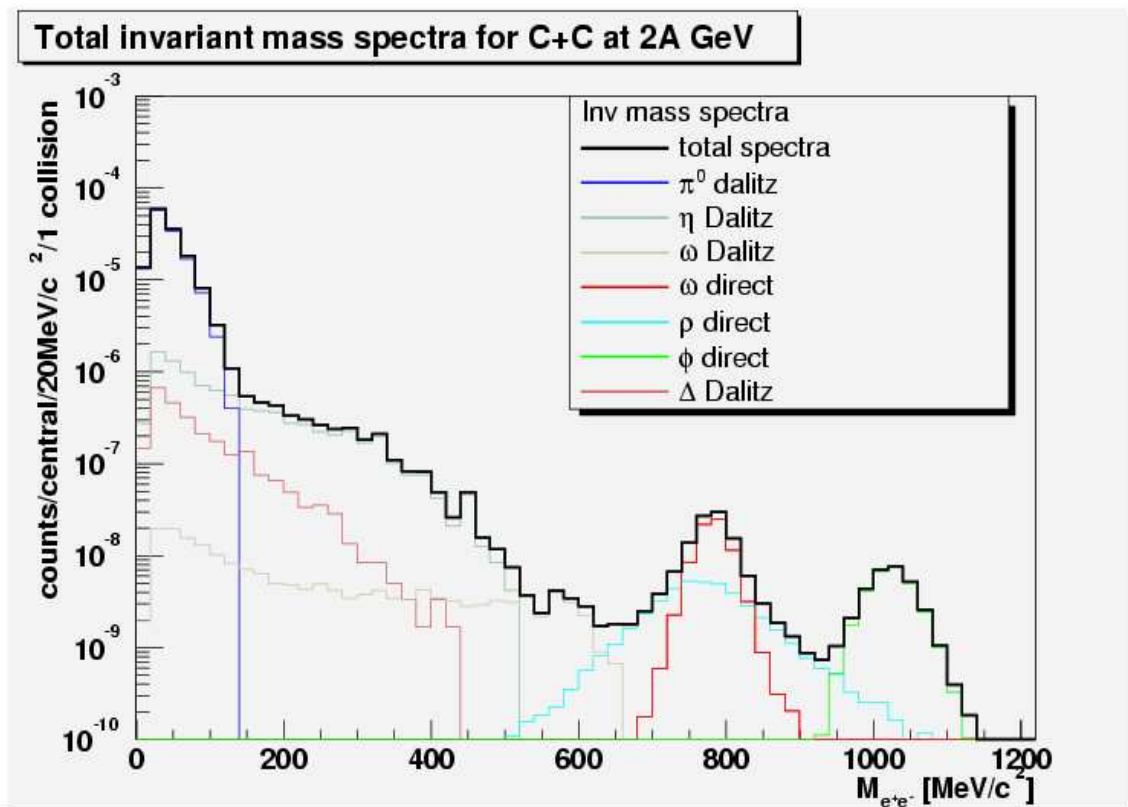


Fig. 3.6: Total invariant mass cocktail for C+C system at 2 A Ge V . Spectrum is normalized for one collision.

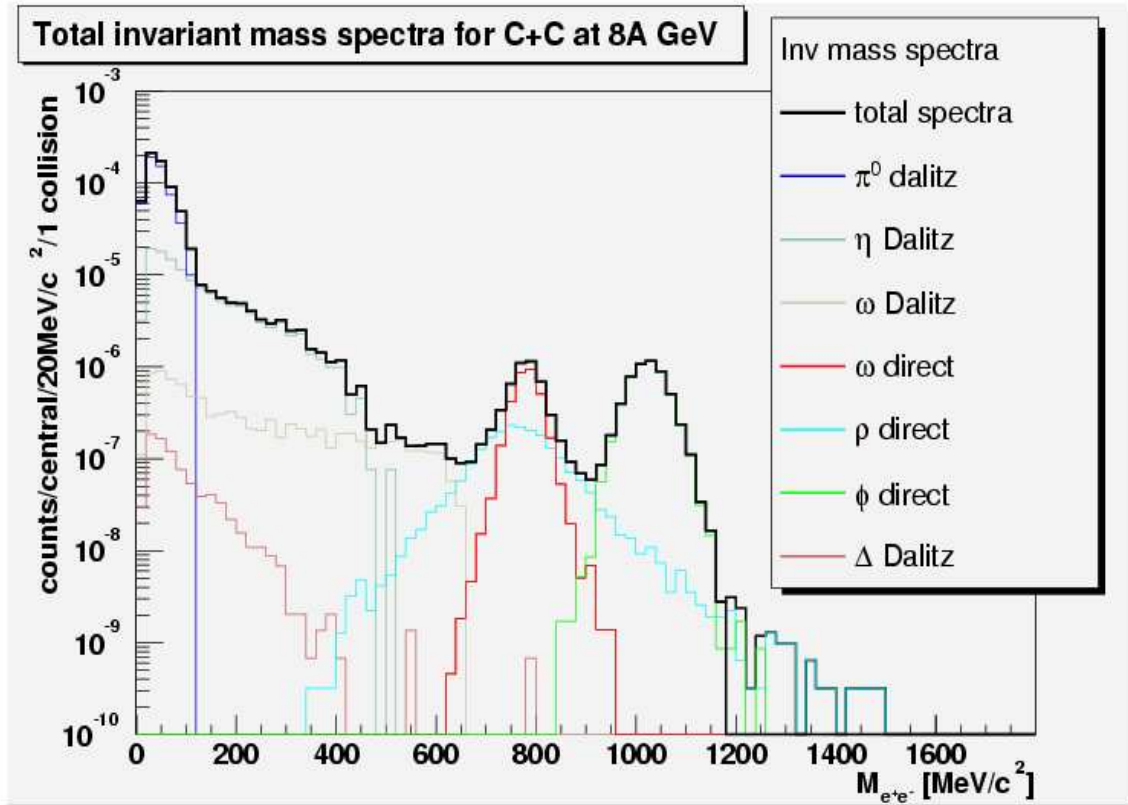


Fig. 3.7: Total invariant mass cocktail for C+C system at 8 A Ge V . Spectrum is normalized for one collision.

Just for a comparison, we will show on Figure 3.8 dilepton cocktail made for The Proposal. This is normalized for 5 days run, i. e. 1.08×10^9 collisions. Quantitative comparison will be done later. This Figure also contains combinatorial background (see below) and *pn-brehmstrahlung*.

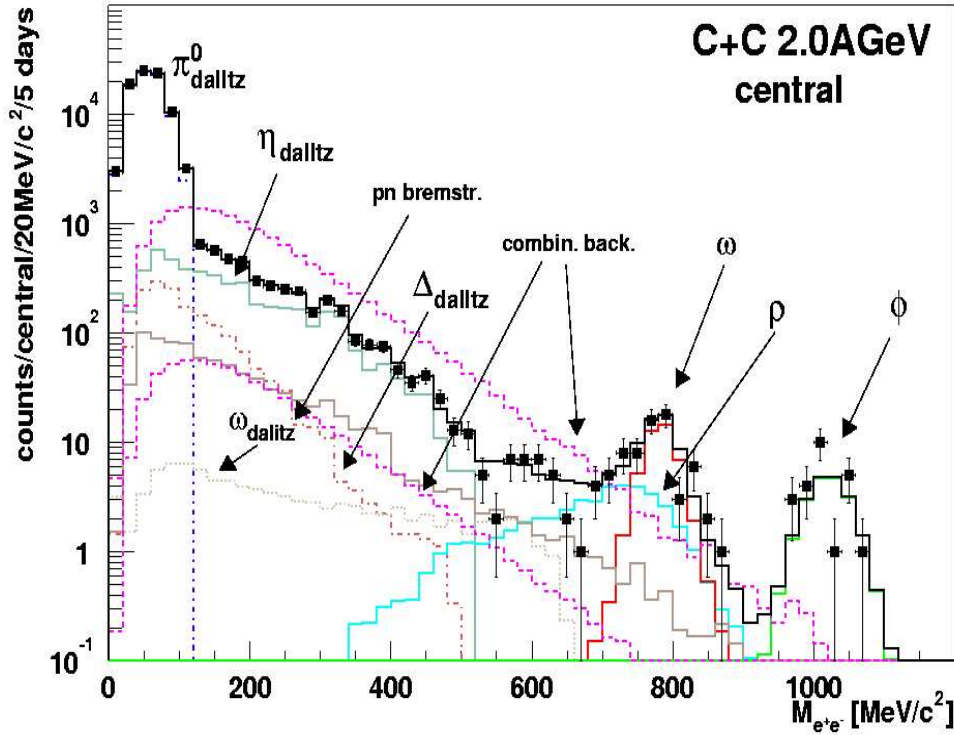


Fig. 3.8: Total invariant mass cocktail for C+C system at 2 A GeV . Normalized for 5 days run. Made for the proposal [Hpr].

3.7 Combinatorial background

As was mentioned above, there is possibility to identify pairs of dileptons, which have no physical meaning, i. e. they are from physically different sources. Therefore our invariant mass spectrum is contaminated by many events, which do not interest us. In the simulation, we have to predict the behavior of this contamination. There are two main methods how to do this task, Unlike-sign pairs and Like-sign pairs. More on this topic can be found in [Lau].

3.7.a Like-sign pairs

This method as well as method below is based on assumption, that electron and positron multiplicity has a Poisson distribution. This technique is based on the fact, that the same event combinatorial like-sign background is identical to the unlike-sign combinatorial background. This needs assumption, that acceptance and efficiency is the same for both electrons and positrons. The result unlike-sign combinatorial background is given by

$$n_{+-}^{l-s} = 2 \cdot \sqrt{n_{++}n_{--}}, \quad (3.7)$$

where n_{++} and n_{--} are spectra of like-sign pairs.

We tried to use this method, but it was clear, that 550 thousand events produced from UrQMD model is not sufficient. It would be necessary to use few order of magnitude larger statistics, but this seems to be too time consuming.

3.7.b Unlike-sign pairs

This method is so called mixed-event method. It means it combines leptons from independent events. The combinatorial background is mixed from unlike-sign pairs that are from different events. Electrons from one event are combined with positrons from another event and vice versa. We have used combination of one-sign leptons with second-sign leptons 80 steps back during iterative process of analyzing. This caused better statistics. We have analyzed 550,000 events produced from UrQMD model. We choosed only pairs with opening angle lower than 5° .

The mixed-event unlike-sign combinatorial background is given by

$$n_{+-}^{ul-s} = \frac{1}{N_{mix}} \frac{1}{N_{evt}} \cdot n_{+-}^{m-e}, \quad (3.8)$$

where N_{mix} is the number of mixed pairs of dileptons, N_{evt} is the number of used events (for normalization to one collision) and n_{+-}^{m-e} is spectrum of mixed-events pairs.

We have used $N_{evt} = 550000$. For 2 A Ge V , I have got $N_{mix} = 2577$ and for 8 A Ge V $N_{mix} = 63799$. Final dilepton cocktails with combinatorial background follow on Figures 3.9 and 3.10.

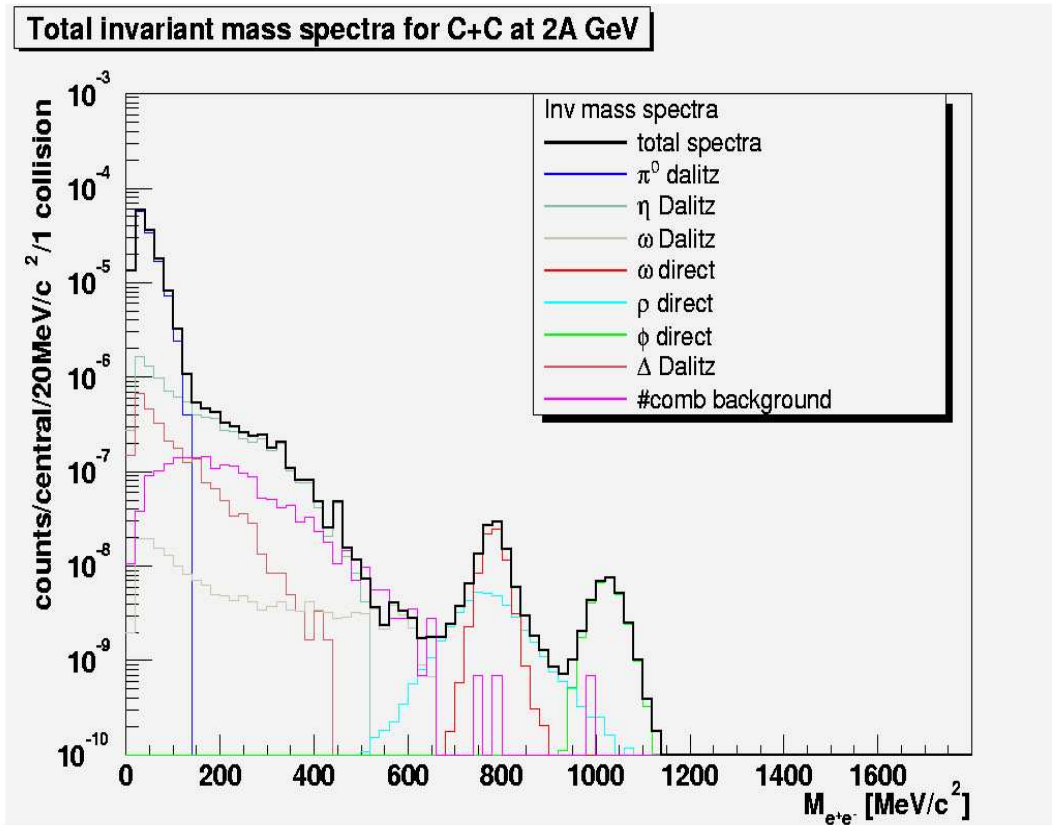


Fig. 3.9: Total invariant mass cocktail for C+C system at 2 A Ge V with combinatorial background included. Spectrum is normalized for one collision.

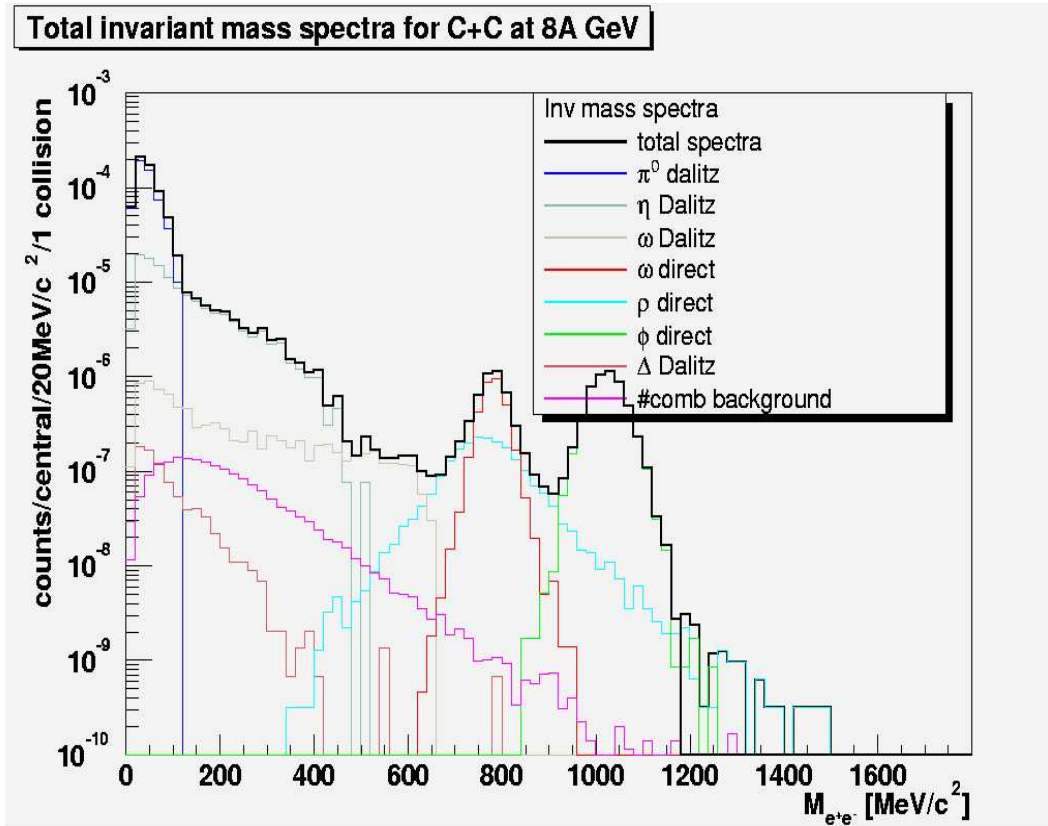


Fig. 3.10: Total invariant mass cocktail for C+C system at 8 A GeV with combinatorial background included. Spectrum is normalized for one collision.

3.8 Acceptance and efficiency

In the previous parts, we have seen total invariant mass spectra of C+C at 2 and 8 A GeV. Information, we need to know, is acceptance of detector setup, i. e. number of pairs, we are able to detect. Acceptance consists of geometrical acceptance and efficiency. In Tables 3.5 and 3.6 we can see result of this for 2 A GeV and 8 A GeV, respectively. In the first column is source, in the second is production multiplicity of dilepton per collision, in the third is detection multiplicity, i. e. number of pairs detected normalized to one collision, in the fourth is the ratio of accepted events to all events produced and in the last column the number of detected events per 5 day run, i. e. 1.08×10^9 collisions.

In these two Tables, we can see visible decreasing of efficiency of detector towards higher incident energies. For ω , ρ and ϕ , events that are physically important, this difference makes around 40%. Just for a comparison in the case of π^0 and Δ , efficiency is roughly the same. On the other hand, in the 8 A GeV energy regime occurs distinct increasing of production of vector mesons, which leads to the total yields growth in the 2 to 3 orders of magnitude. This effect could be seen in in Figure 3.11.

source	$M_{e^+e^-}$	$M_{e^+e^-}^{acc}$	$M_{e^+e^-}^{acc}/M_{e^+e^-}$ [%]	5d run
π^0 Dalitz	2.0×10^{-2}	1.3×10^{-4}	0.65	1.40×10^5
η Dalitz	2.1×10^{-4}	9.1×10^{-6}	4.3	9.82×10^3
ω Dalitz	2.8×10^{-6}	1.8×10^{-7}	6.4	1.94×10^2
ω direct	3.4×10^{-7}	7.4×10^{-8}	21.0	7.99×10^1
ρ direct	2.1×10^{-7}	4.5×10^{-8}	21.0	4.86×10^1
ϕ direct	1.3×10^{-7}	2.9×10^{-8}	22.0	3.13×10^1
Δ Dalitz	8.4×10^{-5}	2.5×10^{-6}	2.9	2.70×10^3

Tab. 3.5: Summarization of results for 2 A Ge V .

source	$M_{e^+e^-}$	$M_{e^+e^-}^{acc}$	$M_{e^+e^-}^{acc}/M_{e^+e^-}$ [%]	5d run
π^0 Dalitz	8.3×10^{-2}	5.2×10^{-4}	0.62	5.61×10^5
η Dalitz	1.6×10^{-3}	5.2×10^{-5}	3.1	5.67×10^4
ω Dalitz	8.6×10^{-4}	4.3×10^{-5}	4.6	4.30×10^4
ω direct	1.1×10^{-4}	1.3×10^{-5}	13.0	1.51×10^4
ρ direct	1.6×10^{-5}	2.1×10^{-6}	13.0	2.26×10^3
ϕ direct	1.5×10^{-5}	1.8×10^{-6}	12.0	2.01×10^3
Δ Dalitz	3.4×10^{-5}	8.2×10^{-7}	2.4	8.85×10^2

Tab. 3.6: Summarization of results for 8 A Ge V .

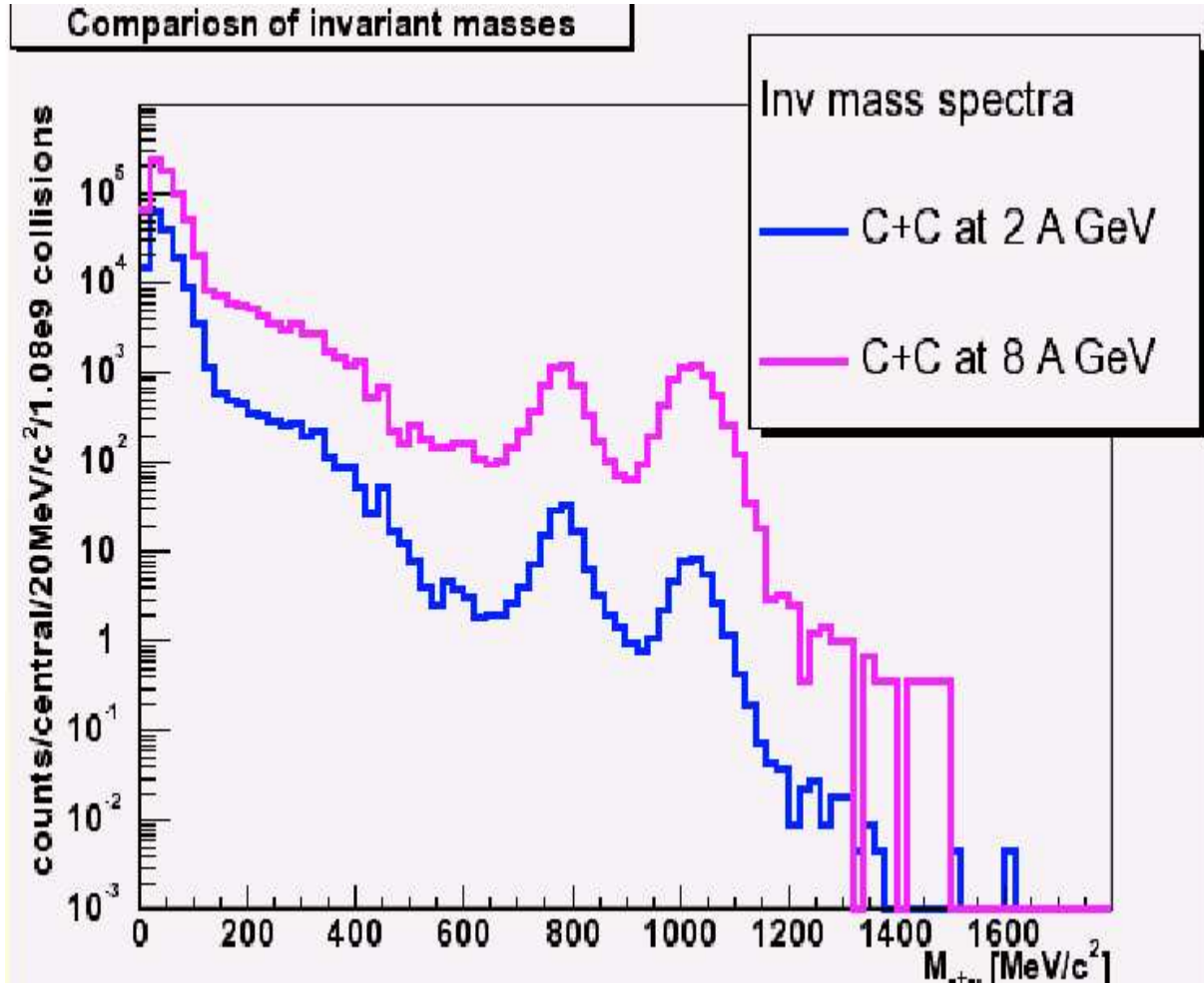


Fig. 3.11: Comparison of total invariant mass cocktails for both energies.

3.8.a Rapidity vs. transversal momentum

More detailed view on the HADES acceptance is via transversal momenta vs. rapidity distribution. Following two pictures represent transversal momenta p_T (x -axis) versus rapidity y (y -axis) distribution. Positrons are in the left column, while electrons are in the right column. First row represents above mentioned distribution directly from thermal model Pluto++. All range of rapidity is visible. In the second row is the same dependency after GEANT and HYDRA processing. Third row represents incorporated analysis acceptance and efficiency.

- 2 A Ge V case: Mid-rapidity region of p_T is around value 0.9. After GEANT and HYDRA processing, we can see significant decrease of events as well cut at approximately $y \approx 1.9$. Acceptance and efficiency uniformly reduce number of events (“lowering pinnacles”). See Figure 3.12.
- 8 A Ge V case: Mid-rapidity region of p_T is around value 1.5. The HADES geo setup causes absolute cut at approximately $y \approx 2$, however, the acceptance around the mid-rapidity region is still around 0.8. This cut leads to systematical losing information in forward rapidity region. Acceptance and efficiency has very similar effect as in previous case. See Figure 3.13.

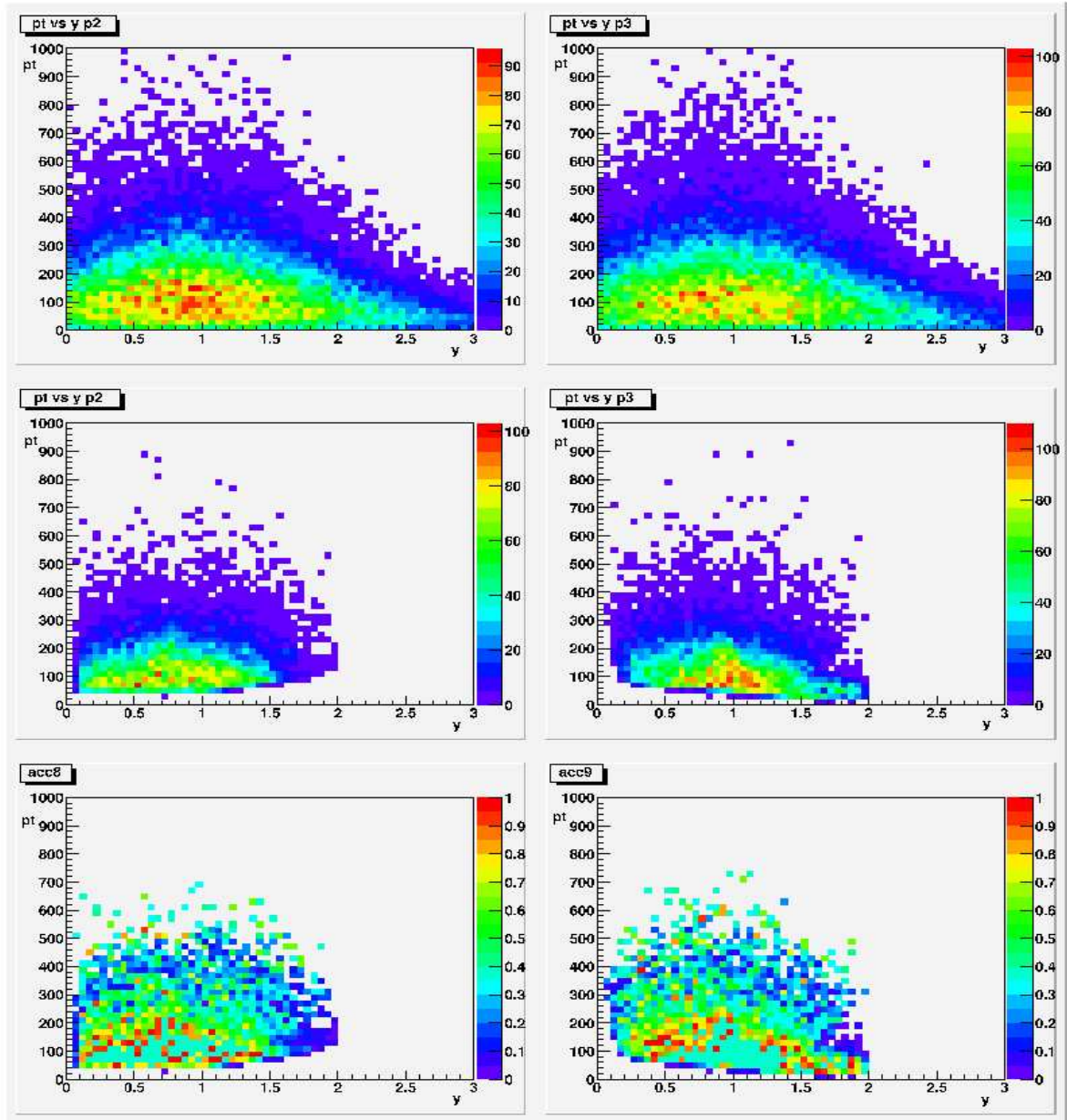


Fig. 3.12: Pt vs y for eta Dalitz channel at 2 A GeV .

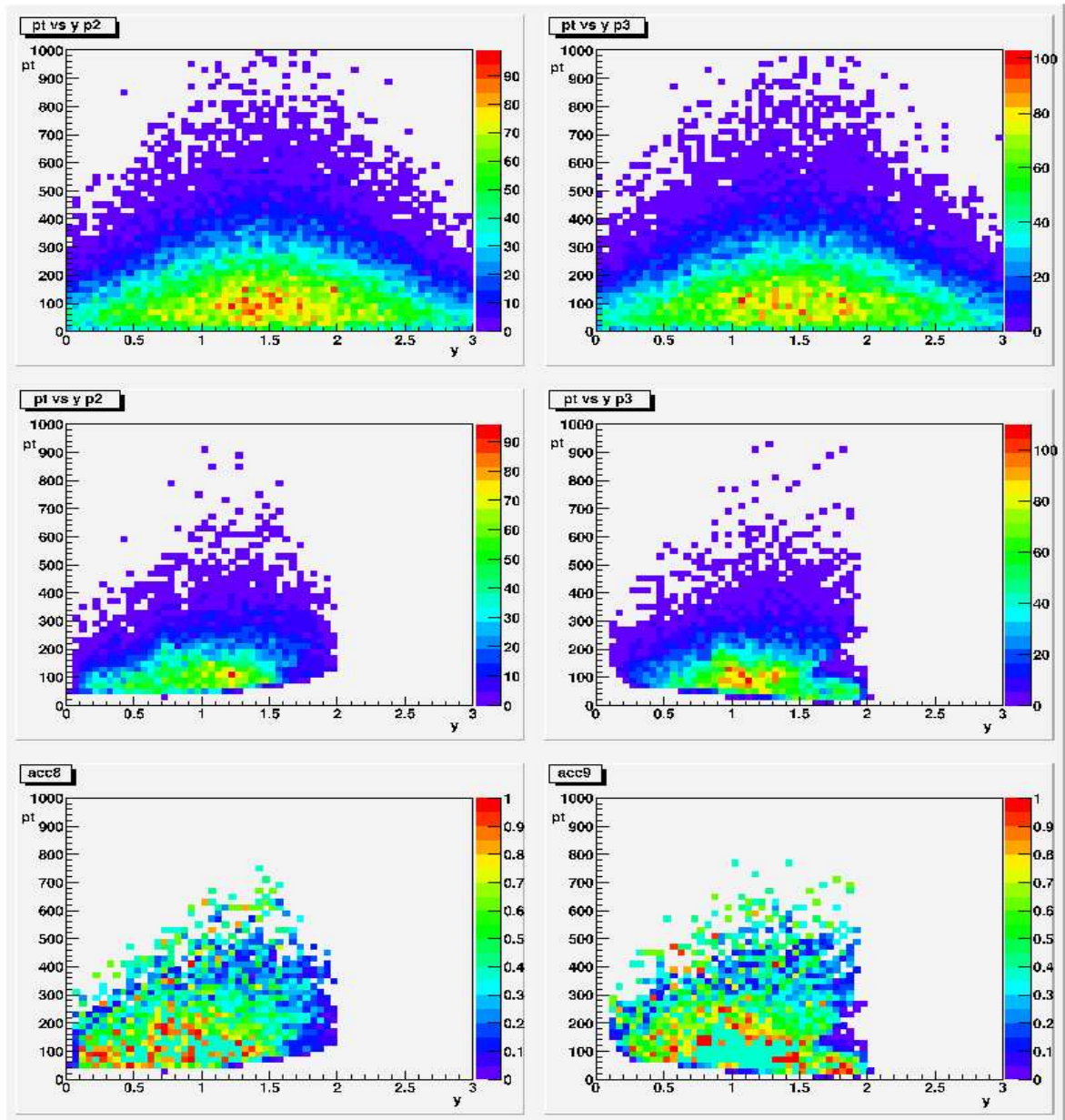


Fig. 3.13: Pt vs y for eta Dalitz channel at 8 A GeV .

Chapter 4

Epilogue

In this chapter the conclusion will be given as well as short comparison with the data from proposal.

4.1 Comparison with The HADES Proposal

We can compare only values for 2A GeV with The Proposal ones. We have got higher yields of registered dilepton pairs. Possible reason is usage of different particle identification method. The quantitative calculation of difference was not done in the frame of this work.

We have also mentioned, that we have used 5° in my constraints. This emerged from the discussion during my work on simulation. [Lau] has value of 15° for simulation process constraint. This different constraints could lead to different yields of particles and therefore to different cocktails.

Next difference could be seen in the shape of the ρ meson. In The Proposal was used theoretical smearing function for the shape of its invariant mass spectra, which simulates change of invariant mass in the dense nuclear medium. This was not repeated in the frame of this work. This is the important physical feature, however, the primary purpose of this work to estimate usefulness of HADES for higher energies of GSI Future Project.

4.2 Conclusion

Higher yields of vector mesons' dilepton pairs is not direct victory. The higher incident energies are accompanied with higher production of hadrons, that also react with detectors. This leads to overfilling of the detector with unwanted events especially in the lower polar angles. This makes the TOFino as inapplicable sub detector in forward regions. The next plans includes replacing of TOFino with newer RPC's walls.

Higher efficiency could be reached with dilatation of the detector in the beam direction. This would lead to better efficiency at lower polar angles.

4.3 Acknowledgment

I would like to thank to Pavel Tlustý, my supervisor, for his invaluable help and to Jaroslav Bielik, presently PhD student at GSI, for his patience and time, he gave me in many talks during my residency at GSI, Darmstadt.

Results of this talk were presented on 6th December 2003 on HADES Collaboration Meeting in Catania, Sicily, and on 9th November 2003 on IEAP CTU seminars course.

Chapter 5

Appendix

In this Chapter, we would like to bring short description of software, we have used for our computation. Everything was done on linux platform. Particular version of given program is mentioned in the Chapter 3, where the description of particular usage of all software tools follows. Then two examples of scripts, we have used, are given.

5.1 Software tools

5.1.a UrQMD

The **Ultra-relativistic Quantum Molecular Dynamics** macroscopic model was designed to describe heavy ion collisions. Main goals are to gain understanding about following physical processes:

- a. Creation of dense hadronic matter at high temperatures
- b. Properties of nuclear matter, Delta & Resonance matter
- c. Creation of mesonic matter and of anti-matter
- d. Creation and transport of rare particles in hadronic matter.
- e. Creation, modification and destruction of strangeness in matter
- f. Emission of electromagnetic probes

More about UrQMD can be found at [Res] or [Urq]. Input of this model are, shortly, incident energy, target and projectile nuclei and impact parameter. Output (in text form) serves as an input for GEANT machinery or can be processed with simple scripts. UrQMD is written in FORTRAN language. Version used in simulation is *v1.2*.

5.1.b Pluto++

Pluto ++ is a standardized tool for HADES simulation purposes. This simulation package consists of a collection of C++ classes, made on modular principles. It can be launched interactively from ROOT environment, and makes use of ROOT and CLHEP-library resources. The focus is on streamlining particle generators by providing features to set up. It also enables manipulating with particles, reaction channels, and complex reactions, as well as applying various filters on the reaction products, such as geometrical and kinematical conditions.

The output can be processed online or used as an input for GEANT. The package includes models for resonance and Dalitz decays, resonance spectral functions with mass-dependent widths, and anisotropic angular distributions for selected channels. Thermal model is also implemented, it enables multi-hadron decays of exploding hot fireballs. Properties of particles are included in a incorporated database. More can be found at [Plt].

5.1.c ROOT

ROOT is an Object Oriented programming environment aimed to process and analyze scientific data from experiments of high energy physics [Roo]. It was developed for NA49 experiment at CERN, where about 10 Terabytes of data was produced per run.

ROOT has built in many useful routines for processing large amount of data, fitting

them with various functions, numerical calculations and imaging results via 2D and 3D histograms.

We cannot mention ROOT without mentioning CINT. CINT is a C++ interpreter used for processing C++ scripts. A CINT script can call compiled parts of code and compiled code can make callbacks to CINT user defined functions and procedures.

5.1.d HYDRA

HYDRA is a package of libraries and methods developed in C++ language for HADES purposes, aimed to reconstruction of events from experiments as well as simulations [Www]. It has also implemented routines for particle identification. HYDRA posses Object Oriented design and cooperate with ROOT environment. His modular structure gives him big variability. It also enables to choose parts of HADES detector, we want to take into mind.

5.1.e GEANT

GEANT is FORTRAN designed Detector Description and Simulation Tool. As the complexity of experiments increases, simulation before experiments become more essential and need to take more care about designing and optimizing detectors, to test reconstruction and analysis programs and last but not least to interpret experimental data. GEANT has his 30th anniversary this year [Gea].

GEANT has an input parameters stored in `*.dat` files used for definition of the detector and conditions, we want to simulate in.

First kind of input are “common” GEANT options, e. g. what kind of interactions of photons with matter we take into mind, what magnetic field we have, how many events we process and others.

Another kind is `*.tup`, which define *ntuples* for every detector subsystem. *ntuple* contains all informations relevant from subsystem point of view, e. g. for TOF detector, there are GEANT event ID, energy loss, time of flight (and few others) stored in TOF *ntuple*.

Next kind are `*.geo` files. These files contain information about geometry setup of the detector and construction facility around and mediae, they are made from.

Last kind of files are `*.hit`. There is stored information about sensitive (or active) volume.

We have used '5% interaction length C target' and 'ideal' geometry. Magnetic field was set on $I = 2500$ A. Example of file for GEANTing of η 's decay products is given at the end of this chapter.

5.2 Examples of scripts

Examples of two scripts follows.

5.2.a Pluto++ example

Example of Pluto++ script for simulation of η Dalitz decay at 8 A GeV and 50000 thousands events, eta_Dalitz.C.

```

#ifndef __CINT__
#include "PParticle.h"
#include "PChannel.h"
#include "PFireball.h"
#include "PReaction.h"
#endif

Float_t Eb = 8.0; // beam energy in AGeV
Float_t T = 0.105; // temperature in GeV
Float_t blast = 0.30; // radial expansion velocity
PFireball *source=new PFireball(" eta",Eb,T,0.,1.,blast,1.0,0.,0.,0.);
source->Print();
PParticle *eta=new PParticle(" eta");
PParticle *s1[ ]=source,eta;
PChannel *c1=new PChannel(s1,1,1);
PParticle* dilep = new PParticle(" dilepton");
PParticle* gamma = new PParticle(" g");
PParticle* ele = new PParticle(" e-");
PParticle* pos = new PParticle(" e+");
PParticle *s2[ ]=eta,dilep,gamma;
PChannel* c2 = new PChannel(s2,2,1);
PParticle *s3[ ]=dilep,ele,pos;
PChannel* c3 = new PChannel(s3,2,1);
PChannel *cc[ ] = c1,c2,c3;
PReaction *r=new PReaction(cc," c8c_eta_dalitz" ,3,0,0,0,1);

r->Print();
r->setHGeant(0);
r->loop(50000);

```

5.2.b GEANT script example

Finally, the example of GEANT script used for processing Pluto++ output follows, c8c_eta_dalitz.dat.

```
PMCF 1
AUTO 1
KINE 0
CKOV 1
FMAP 2
FPOL 0.7215
MXST 25000
SECO 3
JVER 4 1 1
TARG -2.5 2.5 0. 4. 4.
LOSS 1
DRAY 1
TRIG 50000
RUNG 1119 1
SPLIT 2
FILE 1
SWIT 0 0
TIME 0 1000000 1000000
END

/misc/halo/simul/geodat/mediaAll.geo
/misc/halo/simul/geodat/cave_060498.geo
/misc/halo/simul/geodat/sectdb160498.geo
/misc/halo/simul/geodat/coils_230600.geo
/misc/halo/simul/geodat/frames_160498.geo
/misc/halo/simul/geodat/richAprMay01.geo
/misc/halo/simul/geodat/mdc231000.geo
/misc/halo/simul/geodat/showerdb160498.geo
/misc/halo/simul/geodat/tofplustofino_060901.geo
/u/hadesdst/sim/nov01/geant/geodat/target_C_5mm_nov01.geo
/misc/halo/simul/geodat/mdc030398.hit
/misc/halo/simul/geodat/tof221100.hit
/misc/halo/simul/geodat/shower060799.hit
/misc/halo/simul/geodat/rich130698.hit
/tmp/c8c_eta_dalitz.evt
/misc/halo/field/fldrpz_unf.map

kine.tup
rich.tup
mdc.tup
tof.tup
shower.tup

/tmp/c8c_eta_dalitz_geant_50kevt.root
```

References

- [Res] J. Novotny: The Study of Nuclear matter in Heavy-ion Collisions, research work, 2003 Prague
- [Urq] <http://www.th.physik.uni-frankfurt.de/urqmd/>
- [Hpr] The Hades Proposal
- [Hol1] Holzmann R.: The Physics Program of the HADES Experiment at GSI, HADES print server
- [Pos] Pospisil V.: Analyza dat ze studia srazek relativistickyh atomovych jader, research work, 2003 Prague
- [Pdg] <http://pdg.lbl.gov>
- [Plt] <http://www-hades.gsi.de/computing/pluto/html/pluto.html>
- [Gea] <http://wwwasdoc.web.cern.ch/wwwasdoc/pdfdir/geant.pdf>
- [Bss] Bass S. A., Prog. Part. Nucl. Phys. 41 (1998) 225
- [Ant] private communications with Anton Andronic
- [ChSR] Rapp R., Wambach J.: Chiral Symmetry restoration and Dileptons in Relativistic Heavy-Ion Collisions, arXiv:hep-ph/9909229
- [Jar] Bielcik J.: Phd thesis, Technical University Darmstadt 2004
- [Kla] Klay J. L., et. al. (the E895 Collaboration): Charged Pion Production in 2 to 8 A Ge V Central Au+Au Collisions, nucl-ex/0306033 v2
- [Ave] Averbach R. et. al.: Neutral pions and η as probes of the hadonic fireball in nucleus-nucleus collisions around 1 A Ge V , Phys. Rev. C **67**, 024903 (2003)
- [Lau] Fabietti L.: Study of the e^+e^- pair acceptance in the dilepton spectrometer HADES, PhD thesis, 2004 Munich
- [Www] <http://www-hades.gsi.de>
- [Roo] <http://root.cern.ch>